An Analysis of S–T_0 Mixing Polarization of CIDEP in Terms of the Lennard–Jones Fluids: 1-Hydroxy-1-methylethyl Radical in 2-Propanol

Yasutaka Kitahama, Yoshifumi Kimura, and Noboru Hirota*

Department of Chemistry, Graduate School of Science, Kyoto University, Kyoto 606-8502

(Received November 1, 1999)

Calculations of the magnitudes of the polarization (P_{RPM}) due to singlet–triplet (S–T_0) mixing of the radical pair mechanism of chemically induced dynamic electron polarization (CIDEP) are made by numerically solving the stochastic Liouville equations for fluids in which intermolecular interactions are represented by the Lennard–Jones (LJ) potentials. P_{RPM} and the relation between P_{RPM} and the difference in the resonance frequencies of radicals of the pair ($2Q_{ab}$) are examined for the continuum and for various models with different relative strengths of solute–solute, solute–solvent, and solvent-solvent interactions. In the continuum, P_{RPM} reaches the maximum value at small $|J_0|$ (J_0 is the exchange interaction at a distance of the closest approach), and levels off at large $|J_0|$, whereas in the LJ fluids it increases in the region of large $|J_0|$ and reaches a second maximum. At low temperatures, m, which is defined as the exponent in the form of $P_{RPM} \propto Q_{ab}^m$, approaches 0 in the LJ fluids in the region of $|J_0| = 10^{11}$—10^{12} s^{-1}. The calculated results are compared with the experimental results obtained for 1-hydroxy-1-methylethyl radicals in 2-propanol. The main features of the experimental observations are qualitatively better explained by the present models of the LJ fluids than by the continuum with $|J_0| = 10^{11}$—10^{12} s^{-1}. These results are ascribed to the effect of the solvent structure which tends to keep the solvent-separated radical pair for a longer time.

Chemically induced dynamic electron polarization (CIDEP) is the mechanism to produce large electron spin polarizations of transient radicals created by photochemical reactions. CIDEP plays an important role in photochemistry. Two basic mechanisms to produce CIDEP, the radical pair mechanism (RPM)[1,2] and the triplet mechanism (TM),[3,4] were established in the 1970s. In the case of the RPM, pioneering theoretical studies by Pedersen and Freed based on the solutions of stochastic Liouville equation (SLE) showed that the magnitude of the polarization depends strongly on various factors, such as the exchange interaction (J) between the radicals, the difference between the resonance frequencies ($2Q_{ab}$) of the radicals comprising the pair and the diffusion constants (D) of the radicals.[5,6] Shushin derived analytical solutions of the SLE that are applicable to the limiting cases of rapid free diffusion, slow free diffusion, and cage diffusion and predicted very different Q_{ab} dependence of the polarization depending on the type of diffusion.[7] It is desirable to examine these predictions of the theory experimentally, but quantitative analyses of the CIDEP spectra in this regard are not easy, because most CIDEP spectra are complex and do not have sufficiently good signal to noise (S/N) ratios for quantitative analyses.

The CIDEP spectra obtained by irradiation of acetone in 2-propanol (2-PrOH) and acetone-d_6 in 2-PrOH-d_8 appear to be suited for detailed analyses because the spectra are simple involving only one type of radical, and the S/N ratios are high. The photochemical reaction is expressed as

$$(CH_3)_2CO + (CH_3)_2CHOH \rightarrow 2(CH_3)_2\dot{C}OH. \quad (1)$$

The main CIDEP mechanism in this system is the RPM involving the singlet–triplet mixing (ST_0M). In a previous work from this laboratory, it was found that the absolute magnitude of the polarization due to ST_0M–RPM, P_{RPM}, as well as the intensity ratios among the hyperfine peaks of the 1-hydroxy-1-methylethyl radical (HP radical) and 1-hydroxy-1-methylethyl-d_6 radical (HP-d radical) vary significantly with temperature. In order to explain the observed results, Tominaga et al. made an analysis by numerically solving the SLE and concluded that the experimental results could not be explained on the basis of normal diffusion of the radicals.[8,9] They explained the results using a modified diffusion model in which the radicals at close inter-radical distances were assumed to be trapped in the solvent structure and to diffuse more slowly than expected from the normal diffusion. Shushin suggested that the CIDEP spectra of the HP and HP-d radicals could strongly depend on the type of the diffusional motion of the radical.[7] Comparison of the experimental results with his prediction also indicated that the diffusion of the HP and HP-d radicals in 2-PrOH is much slower than expected from the viscosity of the solvent.[10]

In the theoretical analyses of the ST_0M so far made, the solvent has been treated as a structureless continuum. However, in the actual solution the solute molecule diffuses in the structured solvent and this aspect should be properly taken into consideration in the theoretical treatments of the solution

phenomena.[11,12] In the present study, we make an attempt to clarify how the effect of the solvent structure manifests itself in the CIDEP. As a first attempt we consider a simple model system in which the intermolecular interaction is represented by the Lennard–Jones (LJ) potential and the spin properties of the solute molecule are given by those of the HP or HP-*d* radical in 2-PrOH. This model is too simple to reproduce the real system, the HP or HP-*d* radical in 2-PrOH, since the hydrogen bonding may be important in determining the solvent structure around the solute pair in the real system. However, this simple model allows us to calculate the model CIDEP spectra relatively easily, and to test various kinds of parameters, including the solute–solute correlation, in order to extract the determining factors of the CIDEP spectra. To this aim we treat three typical cases for the model system: (i) strong solute–solvent and solute–solute attractive interactions, (ii) normal solute–solvent and solute–solute attractive interactions, (iii) strong solute–solvent but normal solute–solute attractive interactions. Here the term "normal" means that the attractive interaction is the same as that for the solvent molecules. The effect of the solvent structure is included in the SLE by a potential of mean force (PMF). It is shown that the CIDEP spectra for the LJ fluids are significantly different from those obtained by the continuum model.

In the present paper, we first describe the methods of calculation and the models. Then we compare the results of the calculation for the LJ fluids with those for the continuum. In the following section, relevant experimental observations are summarized. There the magnitude of the polarization and its Q_{ab} dependence are the quantities of our interest. Finally we discuss the results for the LJ fluids in comparison with the experimental results. It should be emphasized, however, that the main purpose of this paper is not to make an accurate simulation of the experimental results, but to examine the effects of various solvent structures on the CIDEP signal.

Theoretical Basis of Calculation

The spin dynamics in liquid media can be quantitatively discussed by the SLE in the manner proposed by Freed and Pedersen.[5,6] The SLE is expressed as follows:

$$\frac{\partial \boldsymbol{\rho}}{\partial t} = -i[\mathscr{H}, \boldsymbol{\rho}] + D\Gamma\boldsymbol{\rho}, \tag{2}$$

where $\boldsymbol{\rho}$ is the density matrix of the spin state of the radical pair. $\mathscr{H}$ describes the spin Hamiltonian of the radical pair. D is the mutual diffusion coefficient and Γ is the diffusion operator. Here we have neglected the contribution of the relaxation and the reaction between radicals.

The spin Hamiltonian is given by

$$\mathscr{H} = (g_1\boldsymbol{S}_1 + g_2\boldsymbol{S}_2)\frac{\mu_B\boldsymbol{B}_0}{\hbar} + \sum_i A_{1,i}\boldsymbol{I}_{1,i}\boldsymbol{S}_1 + \sum_j A_{2,j}\boldsymbol{I}_{2,j}\boldsymbol{S}_2 - J(r)\left(2\boldsymbol{S}_1\boldsymbol{S}_2 + \frac{1}{2}\right), \tag{3}$$

$$\langle S \mid \mathscr{H} \mid T_0\rangle = Q_{ab} = \frac{1}{2}\left\{(g_1 - g_2)\frac{\mu_B\boldsymbol{B}_0}{\hbar} + \left(\sum_i A_{1,i}M^a_{1,i} - \sum_j A_{2,j}M^b_{2,j}\right)\right\}, \tag{4}$$

where $A_{1,i}$ is the hyperfine coupling constant of radical 1 due to i th nuclei, $M^a_{1,i}$ is the nuclear magnetic quantum number of radical 1 due to i th nuclei which exists in the overall nuclear spin states a, and the other symbols have the usual meanings. $J(r)$ represents the exchange interaction between the two electron spins $\boldsymbol{S}_1$ and $\boldsymbol{S}_2$, and we employ exponential dependence of $J(r)$ on the inter-radical distance, r,

$$J(r) = J_0\exp[-\alpha(r-d)], \tag{5}$$

where d is a distance of the closest approach and J_0 is the exchange interaction at d.

The diffusion operator, Γ, is expressed as

$$\Gamma = \nabla\cdot[\nabla + (1/k_BT)\nabla U(r)], \tag{6}$$

where the second term in the bracket represents the effect of the solute–solute PMF, $U(r)$. The PMF is expressed in terms of the radial distribution function (RDF) between solute molecules, $g_{xx}(r)$, as:[13]

$$U(r) = -k_BT\ln g_{xx}(r). \tag{7}$$

We assume that the intermolecular interactions are given by the LJ potential,

$$u_{ij}(r) = 4\varepsilon_{ij}\left[\left(\frac{\sigma}{r}\right)^{12} - \left(\frac{\sigma}{r}\right)^{6}\right], \tag{8}$$

where σ is the LJ size parameter and ε_{ij} is the depth of the well. Subscripts represent the species solute x (radical) or solvent s.

We choose SS, ST_0, T_0S, and T_0T_0 as the basis set, because the magnetic field is high enough compared to the total of the hyperfine splittings (hfss). The SLE is conveniently rearranged into a simple form of a vector ρ as

$$\begin{aligned}\rho_1 &= \rho_{SS}\\ \rho_2 &= (\rho_{ST_0} + \rho_{T_0S})/2\\ \rho_3 &= i(\rho_{ST_0} - \rho_{T_0S})/2\\ \rho_4 &= \rho_{T_0T_0}\end{aligned} \tag{9}$$

and the spin Hamiltonian is rewritten as

$$-i[\mathscr{H}, \boldsymbol{\rho}] \rightarrow \begin{pmatrix} 0 & 0 & 2Q_{ab} & 0\\ 0 & 0 & -2J(r) & 0\\ -Q_{ab} & 2J(r) & 0 & Q_{ab}\\ 0 & 0 & -2Q_{ab} & 0\end{pmatrix}\begin{pmatrix}\rho_1\\ \rho_2\\ \rho_3\\ \rho_4\end{pmatrix}. \tag{10}$$

The electron polarization of radical 1 in the overall nuclear state a which interacts with radical 2 in the overall nuclear state b, P_{ab}, is given by

$$P_{ab} = -2\lim_{t\rightarrow\infty} Tr\left\{\int_d^\infty r^2\boldsymbol{\rho}(r,t)\mathrm{d}r\boldsymbol{S}_{1z}\right\}. \tag{11}$$

And the electron polarization of radical 1 in the overall nuclear state a, P_a, is expressed as

$$P_a = \sum_b P_{ab}, \tag{12}$$

It should be noted that $2\rho_2$ corresponds to the electron spin polarization. Assuming that the radicals are generated from the triplet precursor, the ST_0M via Q_{ab} gives rise to nonzero ρ_3 and the effect of $J(r)$ produces ρ_2.

Model and Calculation

The RDF is estimated by the reference hyper-netted chain approximation (RHNC). The calculation procedure was given elsewhere.[14] In the calculation, we used the LJ potential to mimic the state of 2-PrOH as: $\sigma = 0.49$ nm; $\rho^* = 0.82$; $T^* = 0.76$, where ρ^* is a reduced number density and $T^* = k_BT/\varepsilon_{ss}$. The LJ size parameter, σ, is estimated by the viscosity of 2-PrOH gas.[15,16] The values of ρ^* and T^* are determined by the critical density and temperature of 2-PrOH, respectively. Here, for the solvent–solute and solute–solute interactions, the following three cases are considered: (i) $\varepsilon_{sx} = 2\varepsilon_{ss}$ and $\varepsilon_{xx} = 4\varepsilon_{ss}$, (ii) $\varepsilon_{sx} = \varepsilon_{xx} = \varepsilon_{ss}$, (iii) $\varepsilon_{sx} = 2\varepsilon_{ss}$ but $\varepsilon_{xx} = \varepsilon_{ss}$. Figure 1 shows the calculated RDFs. The values of the first peaks of these RDFs are in the order, (i) > (ii) > (iii), as expected from the models. In calculating the temperature dependence of the CIDEP signal, we include the effect of the temperature only in the diffusion constant, and the fluid structure is assumed not to depend on the temperature. This is of course not true in the real system, since the changes of the dynamic properties reflect some kind of structural changes in the fluid. Therefore our calculation should be regarded as a model, only to demonstrate how the change of the diffusion affects the CIDEP signal if the structure is unchanged. The solvent state here is very close to the triple point of the LJ Fluid, and in practice we cannot get the convergence of the integral equation at lower temperatures.

For the dynamic property, we use the parameters to mimic the real system of 2-PrOH, not for the LJ fluid. We use the Stokes–Einstein equation to estimate the mutual diffusion constant

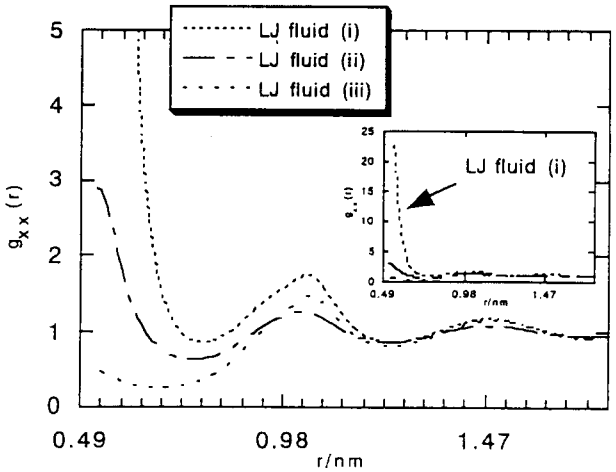

Fig. 1. Three radial distribution functions between solute molecules of LJ fluids for $\sigma = 0.49$ nm; $\rho^* = 0.82$; $T^* = 0.76$; and (i) $\varepsilon_{sx} = 2\varepsilon_{ss}$ and $\varepsilon_{xx} = 4\varepsilon_{ss}$, (ii) $\varepsilon_{sx} = \varepsilon_{xx} = \varepsilon_{ss}$, (iii) $\varepsilon_{sx} = 2\varepsilon_{ss}$ but $\varepsilon_{xx} = \varepsilon_{ss}$.

$$D = 2 \times k_BT/3\pi\eta R, \tag{13}$$

where the viscosity of 2-PrOH is given by[17]

$$\eta/\mathrm{cP} = 4.47 \times 10^{-4} \exp(2532/T), \tag{14}$$

and the hydrodynamic diameter, R, is estimated to be 0.35 nm from the experimentally obtained value of D,[18] since the diffusion constant of the HP radical in 2-PrOH is very similar to the self-diffusion constant of 2-PrOH at room temperature.[19]

In the calculation of the polarization due to ST_0M–RPM, the following parameters are used: $2Q_{ab} = nA_{CH_3} = n \times 1.96$ mT (n = 1—6); or $2Q_{ab} = nA_{CD_3} = n \times 0.29$ mT (n = 1—10) corresponding to the hfss of the HP or HP-d radical, respectively. The value of α is taken as 2×10^{10} m^{-1}. We employ different values of d for different model systems: (i) 0.551 nm; (ii) 0.527 nm; (iii) 0.539 nm. These values are the distances to the first peaks of the RDFs. The value of d is 0.539 nm in the case of the diffusion in the continuum model. The calculation is made by changing J_0 from -10^8 s^{-1} to -10^{13} s^{-1}. The boundary conditions are the same as those used by Freed and Pedersen.[5] The SLE is solved numerically to 400 ns following a published procedure.[20] The value of the polarization due to the ST_0M is constant at 400 ns.

Results and Discussion

1. Results of Calculation. (a) Magnitude of the Polarization. Here we compare the magnitudes of polarization obtained for the LJ fluids with those for the continuum. Figure 2 shows the absolute magnitudes of the polarization due to ST_0M–RPM, P_{RPM}, for $Q_{ab} = 0.58$ mT calculated at different values of $|J_0|$ for the continuum and LJ fluids (i)—(iii). We first note that the solvent structure and the molecular interaction affect the magnitude of the polarization tremendously. These effects depend on $|J_0|$ and temperature. The $|J_0|$ dependence of P_{RPM} in the case of the continuum model is similar to that given by Pedersen and Freed previously.[5,6]

In the region of small $|J_0|$, P_{RPM} increases with an increase of $|J_0|$ and reaches the maximum. In this region, the polarization is mainly developed in the encounter complex. The value of $|J_0|$ to give the maximum value of P_{RPM}, $|J_0(\mathrm{max})|$, is 3×10^{10} s^{-1} at 25 °C and 10^9 s^{-1} at −55 °C in the case of the continuum. In LJ fluid (i), $|J_0(\mathrm{max})|$ becomes about ten times smaller than for the continuum, but it becomes larger on going from LJ fluid (i) to (ii) and (iii). This trend corresponds to the decrease in the first peak of the RDF. In the case of the continuum, Freed and Pedersen noted that $|J_0(\mathrm{max})|$ is obtained from[5]

$$2\tau_1|J_0(\mathrm{max})| \approx 1. \tag{15}$$

where τ_1 is the lifetime for the encounter pair defined by the following equation:

$$\tau_1 = \frac{d}{D\alpha}\left\{1 + (\alpha d)^{-1}\right\}. \tag{16}$$

Then $|J_0(\mathrm{max})|$ is obtained as

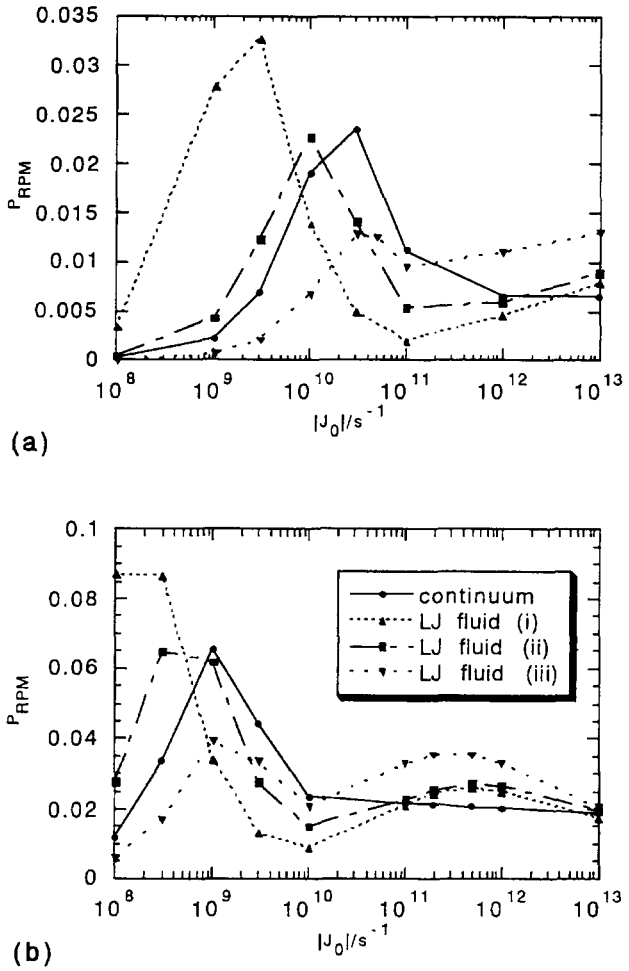

Fig. 2. The calculated absolute magnitude of the polarization due to ST_0M (Q_{ab} = 0.58 mT) as a function of $|J_0|$ at (a) 25 °C and (b) −55 °C in the continuum and the LJ fluids.

$$|J_0(\max)| \approx (2\tau_1)^{-1} = \frac{D\alpha^2}{2(\alpha d+1)}. \quad (17)$$

This equation explains the temperature dependence of $|J_0(\max)|$ and gives 2.5×10^{10} s^{-1} at 25 °C and 7.1×10^8 s^{-1} at −55 °C for the continuum. These values are close to $|J_0(\max)|$ calculated by SLE. The change of $|J_0(\max)|$ in the LJ fluid may be interpreted qualitatively in view of the above equation. We consider the probability that the radical pairs are found in the region of $r < 1.029$ nm (approximately $d+\sigma$) corresponding to the relative distribution of the encounter pairs. This probability shows an approximately exponential decay with a rate constant k_d. Then k_d is considered to be proportional to the microscopic diffusion constant. It increases in the order of (i), (ii), and (iii). The values of k_d for LJ fluid (i) to (iii) are given in Table 1. Assuming that Eq. 17 also holds for LJ fluids, one may predict the order of $|J_0(\max)|$ to be the same as that of k_d. This is in agreement with the results of the SLE calculation. These results indicate that a longer τ_1 (smaller microscopic D) produces a smaller $|J_0(\max)|$. P_{RPM} is expected to increase with a decrease in D.[6] Therefore the value of P_{RPM} in this region is in the order of $P_{RPM}(i) > P_{RPM}(ii) > P_{RPM}(iii)$. It is indicated that a strong solute–solute interaction produces a large polarization in the region of small $|J_0|$. On the other hand, a stronger solvent–solute interaction keeps the radical pair apart and reduces the polarization.

It is to be noted that, in the case of the LJ fluid at −55 °C, there appears a second maximum of P_{RPM} in the region of large $|J_0|$, while in the case of the continuum P_{RPM} levels off at large $|J_0|$ to an asymptotic value which increases with a decrease of D, as already noted by Freed and Pedersen.[5,6] At −55 °C, P_{RPM} shows a second maximum at $|J_0| \approx 5\times10^{11}$ s^{-1} (see Fig. 2b). P_{RPM} at this value of $|J_0|$ is larger for the LJ fluids than for the continuum. Therefore, it is considered that the solvent structure increases polarization at lower temperatures when $|J_0|$ is in the region of 10^{11}—10^{12} s^{-1}. The order of the magnitude of the polarization is $P_{RPM}(i) < P_{RPM}(ii) < P_{RPM}(iii)$, which is the reversed order of the first maximum. The appearances of the second peak in Fig. 2b and of larger values of P_{RPM} in the LJ fluids are likely due to the presence of the second peak of the RDF that keeps the radical pair at the inter-radical distance $r = 2\sigma$ (solvent separated pair). At this distance, the Q_{ab} mixing becomes effective, because the value of J is small and quenching of the Q_{ab} mixing due to large J does not take place. This means that the polarization is produced by simultaneous action of Q_{ab} and J rather than the consecutive action of Q_{ab} and J, as conceived in the reencounter mechanism. A lower probability for a radical pair to stay at longer inter-radical distance may be the cause of a lower value of $P_{RPM}(i)$ than $P_{RPM}(iii)$ at large $|J_0|$.

(b) Q_{ab} Dependence of the Polarization. Adrian's original theory based on the reencounter model predicts a $P_{RPM} \propto Q_{ab}^{1/2}$ relationship for the polarization due to ST_0M,[1] and this equation has been commonly used to analyze CIDEP spectra. However, deviations from the $Q_{ab}^{1/2}$ relationship have been discussed by several groups.[5–7,21] Pedersen and Freed investigated the Q_{ab} dependence of the polarization from the numerical solution of the SLE[5,6] and demonstrated that it is strongly dependent on the value of D.[6] The polarization due to ST_0M is approximately proportional to $(Q_{ab}d^2/D)^l$. For $Q_{ab}d^2/D \leq 0.016$, $l \approx 1/2$ is obtained, but l decreases as $Q_{ab}d^2/D$ becomes larger.[5] On the basis of the analytical solutions of the SLE, Shushin predicted Q_{ab} dependence of the

Table 1. The Decay Rate Constants, k_d, of the Probabilities That the Radical Pairs Are Found in the Region of $r < 1.029$ nm

		Continuum	LJ fluid (i)	LJ fluid (ii)	LJ fluid (iii)
$k_d/10^9$ s^{-1}	at 25 °C	5.9	2.5	5.3	8.4
$k_d/10^8$ s^{-1}	at −55 °C	2.1	0.91	1.9	3.0

polarization due to ST_0M for different types of diffusion.[7] In the case of free diffusion, $P_{RPM} \propto Q_{ab}^{1/2}$ is obtained in the limit of $Q_{ab}d^2/D \ll 1$, but $P_{RPM} \propto Q_{ab}^0$ in the limit of $Q_{ab}d^2/D > 1$. In the case of the cage diffusion with a deep potential well, $P_{RPM} \propto Q_{ab}^{-1}$ is predicted in the limit of $Q_{ab} \gg W_0$, where W_0 is the rate of the phase relaxation.

In the present study, we examine how the Q_{ab} dependence of P_{RPM} depends on $|J_0|$ and D. In order to determine the calculated Q_{ab} dependence of the P_{RPM}, we determine m by fitting the calculated P_{RPM} of the hyperfine lines of the HP and HP-d radicals with an equation: $P_{RPM} = cQ_{ab}^m$. The fitting with a single value of m is satisfactory in most cases. Figures 3 and 4 show examples of the calculated values of m versus $|J_0|$ for the HP and HP-d radicals. The calculated m depends on D as well as $|J_0|$. The $Q_{ab}^{1/2}$ relationship predicted by the reencounter model holds only under limited conditions. In the region of $|J_0| = 10^{11}$—10^{13} s^{-1}, m is 0.3—0.5 at 25 °C, but it decreases at smaller D in both the LJ fluids and the continuum. Therefore the $Q_{ab}^{1/2}$ relationship is approximately correct at room temperature, but it becomes a poor approximation when the diffusion becomes slower.

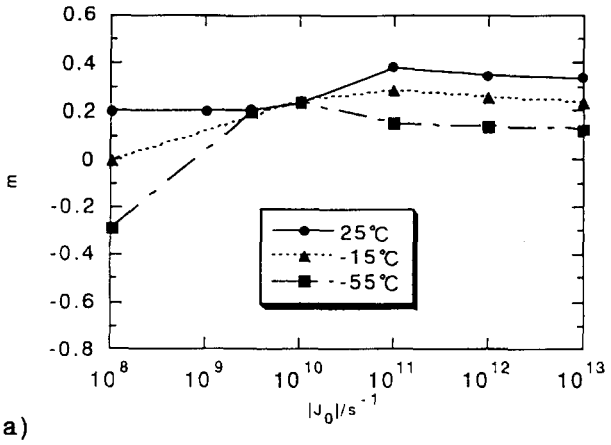

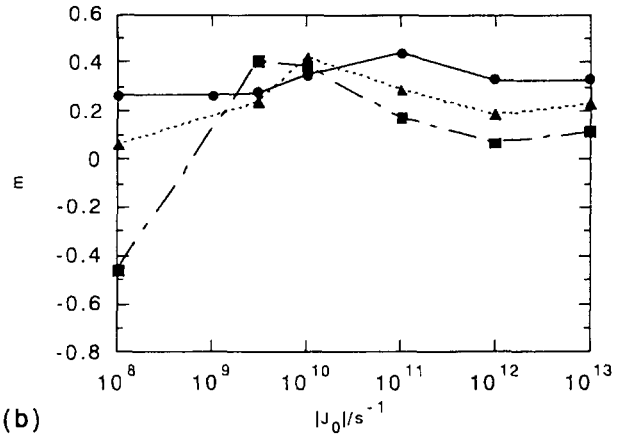

Fig. 3. Q_{ab} dependence of the polarization due to ST_0M as a function of $|J_0|$ for 1-hydroxy-1-methylethyl radical in (a) the continuum and (b) LJ fluid (ii) at 25 °C, −15 °C, and −55 °C. The vertical axis, m, is the power in the equation of the polarization due to ST_0M: $P_{RPM} \propto Q_{ab}^m$.

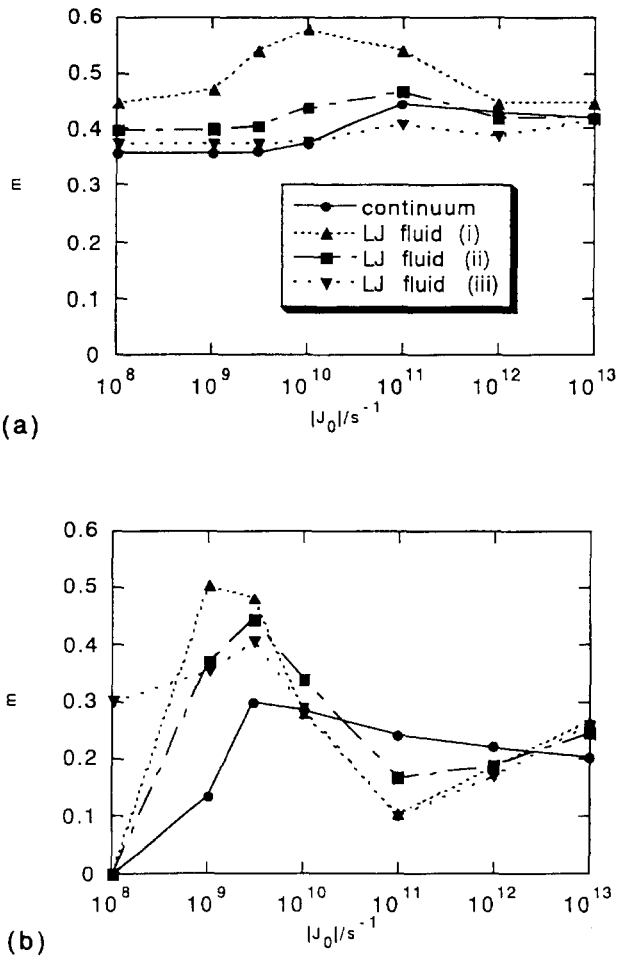

Fig. 4. Q_{ab} dependence of the polarization due to ST_0M as a function of $|J_0|$ at (a) 25 °C and (b) −55 °C for 1-hydroxy-1-methylethyl-d_6 radical in the continuum and the LJ fluids. The vertical axis, m, is the power in the equation of the polarization due to ST_0M: $P_{RPM} \propto Q_{ab}^m$.

The dependence of m on the diffusion is also very sensitive to the value of $|J_0|$. It becomes very small at $|J_0| \approx 3 \times 10^9$ s^{-1} (see Fig. 3). In the region of small $|J_0|$, m becomes temperature dependent again. Furthermore, m becomes even negative at low temperatures. This suggests that the dependence of m on D can be quite different depending on the value of $|J_0|$ of the system.

A somewhat larger dependence of m on D is found for the LJ fluids than for the continuum model, as shown in Figs. 3 and 4. At room temperature, the $|J_0|$ dependence of m is rather small except in the case of LJ fluid (i), where m is somewhat larger at $|J_0| \approx 10^{10}$ s^{-1} (see Fig. 4a). When the diffusion becomes slower, however, m depends strongly on $|J_0|$ as shown in Fig. 4b for the HP-d radical. The $|J_0|$ dependence is also more marked in the LJ fluids than in the continuum; m is larger for the LJ fluids than for the continuum at $|J_0| = 10^9$—10^{10} s^{-1}, but becomes smaller at larger $|J_0|$, 10^{12} s^{-1} for the HP radical (see Fig. 3) and 10^{11} s^{-1} for the HP-d radical (see Fig. 4b). Moreover, m is smaller also at smaller $|J_0|$, 10^8 s^{-1} for the HP radical (see Fig. 3). These results probably reflect the effect of the solvent

structure which tends to keep the radical pair in the regions of effective J mixing for a longer time than in the continuum. Therefore, m for the LJ fluids approaches 0 at $|J_0| = 10^{11}$—10^{12} s^{-1}. In LJ fluid (iii), however, a stronger solvent–solute interaction tends to separate the radical pair. At small $|J_0|$, the J mixing is effective at shorter distances. As shown in Fig. 4b, these may produce a larger value of m in LJ fluid (iii) at $|J_0| = 10^8$ s^{-1}, $m \approx 0.3$, compared with $m \approx 0$ in the other LJ fluids and the continuum.

The dependence of m on D and J_0 are clearly seen in the behaviours of ρ_3 and ρ_2. To produce polarization due to ST_0M, ρ_4 ($= \rho_{T_0T_0}$) must mix with ρ_3 via Q_{ab} and then ρ_3 must mix with ρ_2 via J. In Fig. 5, we show the values of $2\rho_3^*$, $2\rho_3$ in the region of $r < 1.764$ nm, and P_{RPM} calculated by SLE at different temperatures. $2\rho_3^*$ is damped while oscillating in Q_{ab} frequency between positive and negative values. The damping constant depends on J and D. At room temperature, fast diffusional motion controls the damping rates of $2\rho_3^*$, as shown in Fig. 5a. Thus the damping rates of $2\rho_3^*$ are similar in all the regions of $|J_0|$, resulting in similar values of m at 25 °C irrespective of the values of $|J_0|$. The polarization of a radical with larger Q_{ab} is larger than that of a radical with smaller Q_{ab}, as indicated in Fig. 5a. When the diffusion becomes slower, the damping rate of $2\rho_3^*$ becomes low (see Fig. 5b). Small $|J_0|$ also makes the damping rate of $2\rho_3^*$ lower, as shown in Fig. 5b, because the mixing of ρ_3 with ρ_2 via smaller J is slower. In this case, the polarization of a radical pair with larger Q_{ab} may become smaller than that of a radical with smaller Q_{ab}, making m negative, as shown in Fig. 5b. In the case of large $|J_0|$, the polarizations of both radicals are similar and m becomes close to 0.

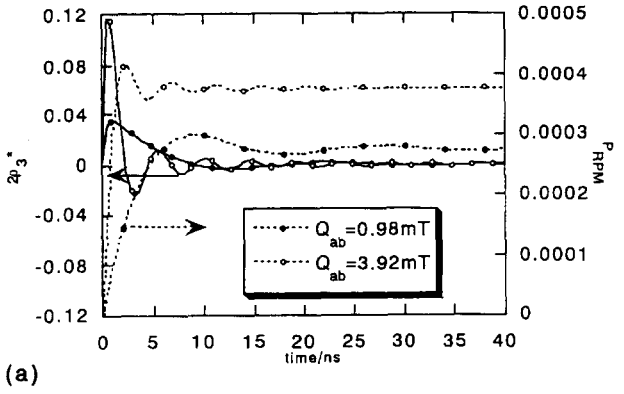

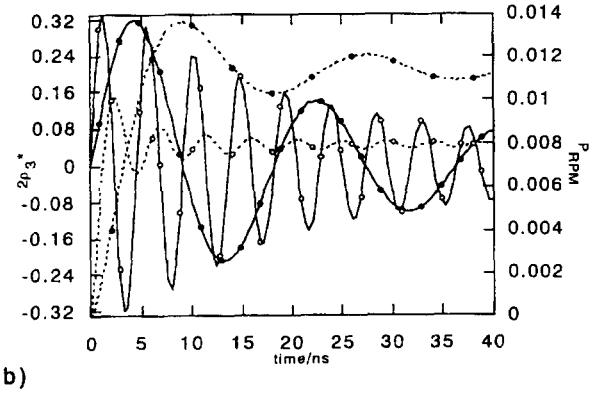

Fig. 5. Time profiles of $2\rho_3^*$, where $2\rho_3^*$ is the values of $2\rho_3$ in the region of $r < 1.764$ nm, and P_{RPM} for 1-hydroxy-1-methylethyl radical in the continuum at (a) $J_0 = -10^8$ s^{-1} and 25 °C ($m \approx 0.2$), and (b) $J_0 = -10^8$ s^{-1} and −55 °C ($m \approx -0.3$). The solid lines show the time profiles of $2\rho_3^*$ and the dotted lines show the time profiles of P_{RPM}.

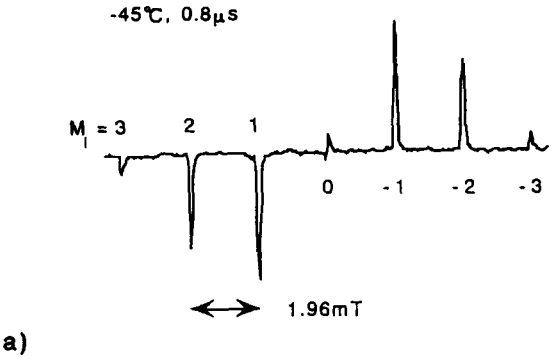

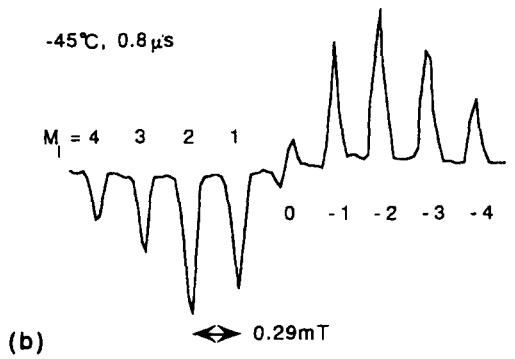

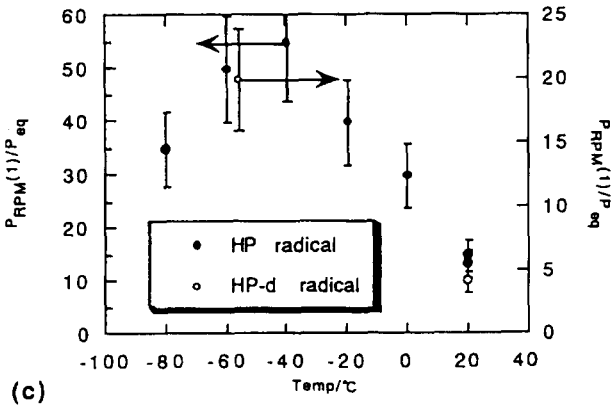

Fig. 6. The CIDEP spectra observed at −45 °C and 0.8 μs after laser pulse for (a) 1-hydroxy-1-methylethyl radical and (b) 1-hydroxy-1-methylethyl-d_6 radical. (c) The ratios of the absolute magnitude of the polarization of the $M_I = \pm 1$ peak due to ST_0M, $P_{RPM}(1)$, to that at thermal equilibrium, P_{eq}, for these radicals. Here M_I is the nuclear spin magnetic quantum number.

Negative m can be understood qualitatively in the following way. As seen in Fig. 5, ρ_3^* may be approximately given by the following equation:

$$2\rho_3^*(t) \propto \sin(Q_{ab}t)\exp(-bt), \tag{18}$$

where b is the damping constant. Assuming that J is constant in the region of effective mixing, P_{RPM} is given as

$$P_{RPM} \propto J\int_0^\infty \sin(Q_{ab}t)\exp(-bt)dt = \frac{JQ_{ab}}{Q_{ab}^2+b^2}. \tag{19}$$

Then the Q_{ab} dependence is determined by the relative values of Q_{ab} and b. When Q_{ab} is much larger than b, m can be negative. In the limit of $Q_{ab} \gg b$, $P_{RPM} \propto Q_{ab}^{-1}$ is obtained. On the other hand, in the limit of $Q_{ab} \ll b$, $P_{RPM} \propto Q_{ab}$. It is noted that these limiting relations are the same as those obtained by Shushin's cage diffusion model.[7]

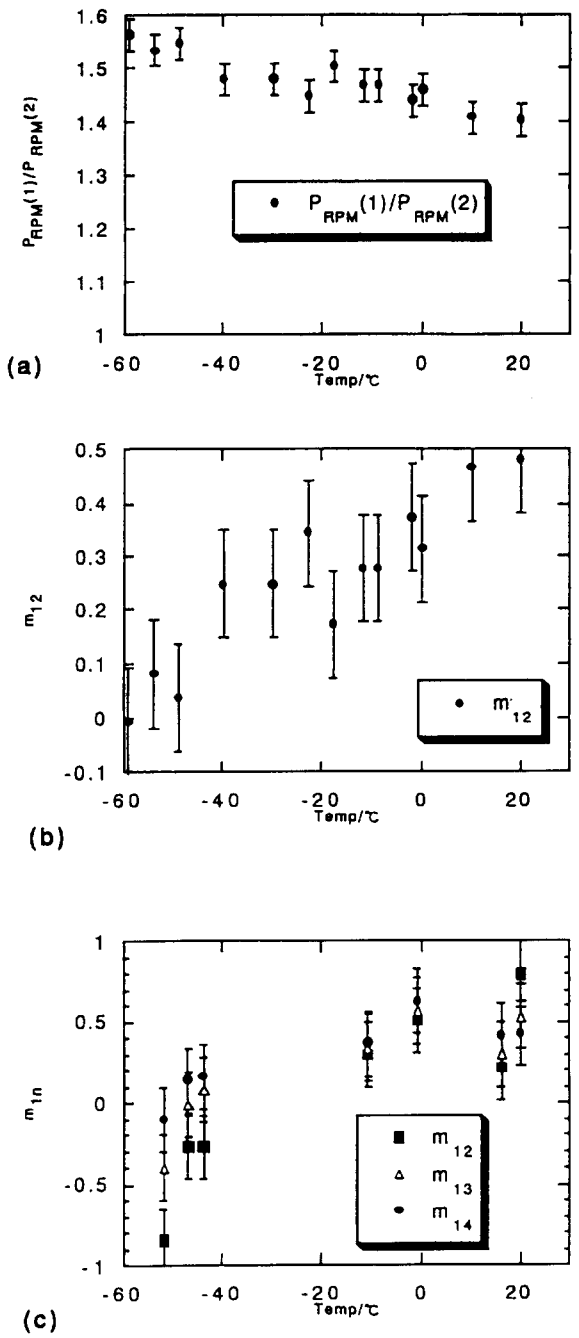

Fig. 7. (a) The relative intensities of the each hyperfine line of 1-hydroxy-1-methylethyl radical at various temperatures. The estimated values of m_{1n} from the observed ratios of $M_I = \pm 1$ peak to $M_I = \pm n$ peak of (b) 1-hydroxy-1-methylethyl radical and (c) 1-hydroxy-1-methylethyl-d_6 radical at various temperatures. Here m is the power in the equation of the polarization due to ST_0M: $P_{RPM} \propto Q_{ab}{}^m$.

2. Experimental Results and Analysis. Here we summarize the relevant experimental observations on the CIDEP spectra of the HP and HP-d radicals. The data are taken mostly from the previous work,[8] but we have made additional experiments to confirm the results.[22] The representative CIDEP spectra are shown in Figs. 6a and 6b. The spectra consists of well separated hyperfine lines due to the interactions with the protons or deuterons in the methyl groups. The splittings are 1.96 and 0.29 mT in the HP and HP-d radicals, respectively. In the case of the HP radical, each hyperfine line is further split by the OH proton splitting, which varies from 0.07 mT at 25 °C to nearly zero at −30 °C and then to 0.03 mT at −60 °C. Under high resolution conditions, splittings due to the second order effect of the hyperfine interaction are observable in the HP radical.[23]

The magnitudes of the polarizations of the HP and HP-d radicals were previously determined at various temperatures from the analyses of the time profiles of the CIDEP signals obtained by using the CW- and FT- time-resolved EPR techniques.[8,24,25] Figure 6c shows the temperature dependence of the values of $P_{RPM}(1)/P_{eq}$, where $P_{RPM}(1)$ and P_{eq} are the polarizations of the $M_I = \pm 1$ peaks due to the ST_0M and those at thermal equilibrium, respectively. The experimental values of $P_{RPM}(1)/P_{eq}$ are strongly temperature dependent and the value has a maximum at around −40 °C for the HP radical. The maximum values are about 55 for the HP radical and 20 for the HP-d radical, respectively.

In the previous work, it was noted that the intensity ratios of the ST_0M polarizations of the hyperfine lines are temperature dependent.[8] The ST_0M polarization is easily obtained by taking 1/2 of the difference of the peak intensities of the $+M_I$ and $-M_I$ peaks ($M_I = 1$ and 2). Figure 7a shows the temperature dependence of the intensity ratio between $P_{RPM}(1)$ and $P_{RPM}(2)$ of the HP radical estimated from the integrated intensities of the hyperfine lines measured at 0.8 μs after laser excitation. This dependence is also confirmed from the measurement of the peak intensities. At a delay time of 0.8 μs, the splittings due to the OH proton and the second order hyperfine interaction are not resolved, but they mainly determine the linewidth. The M_I dependent line broadening is not significant over the temperature regions of our interest. We have also confirmed that the polarization ratio is constant over the delay times of 0.5—2.0 μs. At longer times, serious deviations arise because of the contributions due to the free pair and the effect of the cross relaxation. At very low temperatures, overlapping with the radical pair spectrum becomes a source of error. The ST_0M polarization ratios are also estimated for the HP-d radical from the peak intensities

at 0.8 μs, where the effects of the OD splitting and the second order splittings are negligible in the linewidth because of the small nuclear magnetic moment of the deuteron. The M_I dependent line broadening is also negligible. However, overlapping with the radical pair spectrum prevents us from making accurate estimations at low temperatures.

We now analyze the observed ratios[8,10] in terms of the value of m in the equation, $P_{RPM} \propto Q_{ab}^m$. The ST_0M polarization of a particular hyperfine line of a radical is given from the degeneracies of nuclear spin states of the a and b radicals of the pair and the difference in the resonance frequencies of two radicals. In the case of the HP radical, the ratio between $P_{RPM}(1)$ and $P_{RPM}(2)$ is given by

$$P_{PRM}(1)/P_{PRM}(2) = \frac{15\{(2A_{CH_3})^m + 6(3A_{CH_3}/2)^m + 14A_{CH_3}^m + 14(A_{CH_3}/2)^m\}}{6\{(5A_{CH_3}/2)^m + 6(2A_{CH_3})^m + 15(3A_{CH_3}/2)^m + 20A_{CH_3}^m + 14(A_{CH_3}/2)^m\}} \quad (20)$$

Similar equations are obtained for three sets of peaks of the HP-*d* radicals. Numerically solving the equations for m with the experimentally obtained ratios, we estimate the values of m. The values determined in this way are given in Fig. 7. Here m_{12}, m_{13}, and m_{14} are obtained from $P_{RPM}(1)/P_{RPM}(2)$, $P_{RPM}(1)/P_{RPM}(3)$, and $P_{RPM}(1)/P_{RPM}(4)$, respectively. The value of m is quite temperature dependent: in the HP radical, m is about 0.5 at room temperature but decreases gradually and reaches 0 at −60 °C. In the HP-*d* radical, a similar trend is also found, though the values of m obtained by different sets of peaks are somewhat scattered at low temperatures.

3. Comparison of the Calculated Results with the Experimental Ones. We now compare the model calculation results with the experimental ones on the HP and HP-*d* radicals. It was previously noted that the observed polarization of the HP radical could not be explained with the normal diffusion using the continuum model.[8,9] In Table 2, we show the values of the model calculation for $P_{RPM}(1)/P_{eq}$ of the HP and HP-*d* radicals. When $|J_0|$ is in the range of 10^{11}—10^{12} s^{-1}, the values of $P_{RPM}(1)/P_{eq}$ at −55 °C are considerably larger than those at 25 °C for all cases. This trend is in agreement with that found experimentally. In this range of $|J_0|$, the ratios between $P_{RPM}(1)/P_{eq}$ at 25 °C and those at −55 °C are larger for the LJ fluids than for the continuum, namely, the temperature dependence of the polarization due to ST_0M is stronger in the LJ fluids than in the continuum. The largest values of $P_{RPM}(1)/P_{eq}$ are obtained for LJ fluid (iii), which are 27 in HP radical and 15 in HP-*d* radical at −55 °C. Therefore, the results obtained for the LJ fluids with these $|J_0|$ values, particularly those for (iii), are in better agreement with the experimental results than for the continuum. On the other hand, when $|J_0|$ is 10^{10} s^{-1} or smaller, the calculated values of $P_{RPM}(1)/P_{eq}$ at 25 °C are often larger than those at −55 °C, which is inconsistent with the experimental results.

In the region of large $|J_0|$, P_{RPM} monotonously increase with a decrease of D in the continuum.[6] In the LJ fluids, however, since P_{RPM} shows a second maximum, $P_{RPM}(1)$ may increase and then decrease at lower temperature. This is also consistent with the experimental result. One can conclude that the ST_0M polarizations observed in the HP and HP-*d* radicals are qualitatively well explained with $|J_0| = 10^{11}$—10^{12} s^{-1} and a model of the LJ fluid with a stronger solute–solvent interaction.

Experimentally, m was found to decrease from 0.5 at room temperature to 0 at −60 °C. This trend of the decrease was also reproduced qualitatively in the region of $|J_0| = 10^{11}$—10^{13} s^{-1}, but the calculated changes are smaller than the observed ones. The calculated m also never reaches 0 in this range of $|J_0|$. Although better agreements are obtained with the LJ fluids than with the continuum, improvements obtained by the use of the LJ fluids are rather small.

The calculation indicates that the temperature dependence of m is very sensitive to the value of $|J_0|$. It becomes very small at $|J_0| = 3\times10^9$ s^{-1} (see Fig. 3). It has been noted that the temperature dependence of the Q_{ab} dependence of the CIDEP spectrum of the *t*-butyl radical obtained by the

Table 2. The Calculated Absolute Magnitude of the Polarization of the $M_I = \pm1$ Peak Due to ST_0M for 1-Hydroxy-1-methylethyl (HP) Radical and 1-Hydroxy-1-methylethyl-d_6 (HP-*d*) Radical in the Continuum and the LJ Fluids

	HP radical			
	Continuum	LJ fluid (i)	LJ fluid (ii)	LJ fluid (iii)
25 °C at $\|J_0\|=10^{11}$ s^{-1}	13	2.7	6.5	10
−55 °C at $\|J_0\|=10^{11}$ s^{-1}	20	16	19	27
25 °C at $\|J_0\|=10^{12}$ s^{-1}	7.3	5.3	6.5	11
−55 °C at $\|J_0\|=10^{12}$ s^{-1}	18	20	22	26
	HP-*d* radical			
	Continuum	LJ fluid (i)	LJ fluid (ii)	LJ fluid (iii)
25 °C at $\|J_0\|=10^{11}$ s^{-1}	4.4	0.81	2.2	3.8
−55 °C at $\|J_0\|=10^{11}$ s^{-1}	9.4	9.8	10	15
25 °C at $\|J_0\|=10^{12}$ s^{-1}	2.7	1.9	2.4	4.5
−55 °C at $\|J_0\|=10^{12}$ s^{-1}	8.9	11	12	15

photolysis of di-*t*-butylketone in 2-PrOH is rather small, and the spectrum can be explained well by the $Q_{ab}{}^{1/2}$ relationship down to very low temperatures.[10,26] In view of the present result, it seems possible that the $|J_0|$ value of the bulky *t*-butyl radical is much smaller than that of the HP radical and that *m* is rather insensitive to the temperature.

Summary and Concluding Remarks

The following are the main results obtained by the present calculation.

(1) The maximum value of P_{RPM} in the region of small $|J_0|$ strongly correlates with the intensity of the first peak of RDF, which is an indication of the stability of the contact radical pair.

(2) In the LJ fluids, P_{RPM} increases in the region of large $|J_0|$ and reaches a second maximum at $|J_0| = 10^{11}$—10^{12} s^{-1} and -55 °C. This result is ascribed to the presence of the solvent-separate pair in the region of effective *J* mixing.

(3) The Q_{ab} dependence of the polarization expressed in the form of $P_{RPM} \propto Q_{ab}^{m}$ depends on $|J_0|$ as well as temperature. At $|J_0| = 10^{11}$—10^{12} s^{-1}, *m* is 0.3—0.5 at room temperature irrespective of the models, but it approaches 0 in the LJ fluids at lower temperatures.

(4) When $|J_0|$ is small, *m* can be negative at low temperatures. At $|J_0| \approx 3\times10^{9}$ s^{-1}, temperature dependence of *m* is rather small.

It is shown that the CIDEP due to the ST_0M–RPM is strongly influenced by the solvent structure and molecular interaction. The main features of the experimental results on the HP and HP-*d* radicals are qualitatively better explained by the present models of the LJ fluids than by the continuum with $|J_0| = 10^{11}$—10^{12} s^{-1}. The calculated results for the LJ fluids are not in quantitative agreement with the observed results, but it is encouraging to see that the inclusion of the solvent structure leads to a considerably better agreement with the experimental results even with such a crude model. Tominaga et al. previously could reproduce the experimental results by assuming very slow diffusion for radicals in the pair, which was thought to be brought about by the caged structure of the solvent due to hydrogen bonding.[8,9] If the effects of specific molecular interactions such as hydrogen bonding are taken into consideration, further improvements may be expected.

References

1 F. J. Adrian, *J. Chem. Phys.*, **54**, 3918 (1971).

2 R. Captein, *J. Am. Chem. Soc.*, **94**, 6251 (1972).

3 P. W. Atkins and G. T. Evans, *Mol. Phys.*, **27**, 1633 (1974).

4 J. B. Pedersen and J. H. Freed, *J. Chem. Phys.*, **62**, 1706 (1975).

5 J. H. Freed and J. B. Pedersen, *Adv. Magn. Reson.*, **8**, 1 (1976).

6 J. B. Pedersen and J. H. Freed, *J. Chem. Phys.*, **58**, 2746 (1973).

7 A. I. Shushin, *Chem. Phys. Lett.*, **170**, 78 (1990).

8 K. Tominaga, S. Yamauchi, and N. Hirota, *J. Chem. Phys.*, **92**, 5175 (1990).

9 N. Hirota, K. Tominaga, and S. Yamauchi, *Bull. Chem. Soc. Jpn.*, **68**, 2997 (1995).

10 N. Hirota, Y. Miura, K. Ohara, and M. Terazima, "Modern Applications of EPR/ESR, Proceeding of the First Asia-Pacific EPR/ESR Symp.," Abstr., p. 114 (1998).

11 K. Ibuki and M. Ueno, *J. Chem. Phys.*, **107**, 6594 (1997).

12 S. H. Northrup and J. T. Hynes, *J. Chem. Phys.*, **71**, 871 (1979).

13 See, for example: J. P. Hansen and I. R. McDonald, "Theory of Simple Liquids," 2nd ed, Academic Press, London (1986).

14 Y. Kimura and Y. Yoshimura, *Mol. Phys.*, **72**, 279 (1991).

15 D. C. Reid, J. M. Prausnitz, and B. E. Poling, "The Properties of Gases and Liquids," 4th ed, McGrow-Hill, New York (1987), pp. 392—404.

16 K. Stephan and K. Lucas, "Viscosity of Dense Fluids," Plenum, New York (1979), p. 225.

17 T. Tonomura, *Sci. Rep. Tohoku Imp. Univ. Ser. 1*, **22**, 104 (1933).

18 K. C. Pratt and W. A. Wakeham, *J. Chem. Soc., Faraday Trans. 2*, **73**, 997 (1977).

19 M. Terazima, K. Okamoto, and N. Hirota, *J. Phys. Chem.*, **97**, 13387 (1993).

20 Y. Kitahama and H. Murai, *Chem. Phys.*, **238**, 429 (1998).

21 K. A. McLauchlan and D. G. Stevens, *J. Magn. Reson.*, **63**, 2367 (1985).

22 The experimental setup and procedure are the same as those described in Ref. 8.

23 K. Tominaga, S. Yamauchi, and N. Hirota, *J. Chem. Phys.*, **88**, 553 (1988).

24 H. van Willigen, P. R. Levstein, and M. H. Ebersole, *Chem. Rev.*, **93**, 173 (1993).

25 K. Tominaga, S. Yamauchi, and N. Hirota, *Chem. Phys. Lett.*, **149**, 32 (1988).

26 N. Hirota and S. Yamauchi, "Dynamic Spin Chemistry," ed by S. Nagakura, H. Hayashi, and T. Azumi, Kodansha, Tokyo (1998), pp. 223—226.